THE BELL SYSTEM TECHNICAL JOURNAL
Vol. 53, No. 4, April 1974
Printed in U.S.A.

An Optical Repeater With High-Impedance Input Amplifier

By J. E. GOELL

(Manuscript received September 14, 1973)

A 6.3-Mb/s repeater for fiber optic communication systems is described which incorporates a high-impedance input amplifier. It is shown that by utilizing an input circuit with a time constant which is long compared to the bit interval and equalizing after the signal has been sufficiently amplified to set the signal-to-noise ratio, thermal noise can be decreased. As a result, a reduction can be realized in the required signal and, with an avalanche detector, in the optimum gain.

The repeater, which was realized in a compact form employing standard integrated circuits, utilizes a GaAs light-emitting diode as its optical source. Other features include automatic gain and threshold controls and recovered timing.

I. INTRODUCTION

Digital communication systems utilizing low-loss optical fibers are presently being investigated. The realization of fibers with losses as low as 4 dB/km[1] has opened the way for numerous applications. System configurations will depend on such factors as fiber dispersion, fiber cost, desired information capacity, and terminal costs. Transmission rates near 6.3 Mb/s are attractive because fiber group delay dispersion is not expected to be a problem even with an incoherent source, and a wide variety of low-cost integrated circuits are applicable. If, as now appears likely, the fiber cost is low, then space multiplex could be an attractive alternative to time multiplex in achieving high capacity.

The repeater described here incorporates a high-impedance input amplifier which is similar in approach to ones that have been used for other applications incorporating a capacitive detector such as nuclear particle counters[2] and television cameras.[3] As a result of the high-input

impedance, the power required to achieve a specified error rate is reduced, as is the optimum gain if an avalanche detector is used. The latter advantage is important since it eases the fabrication of the detector diode and increases its thermal stability.

The repeater employs return-to-zero pulses with 50-percent duty cycle. The only word pattern restriction is that an occasional "one" be included so timing can be recovered and signal level can be determined. The optical signal is generated by a gallium arsenide light-emitting diode (LED) operating at 0.9 μ wavelength.[4] Diodes of the type employed have been built with output powers of up to about 5 mW. Optical powers to 1 mW have been coupled from these diodes into a fiber with a 0.63 numerical aperture. The repeater was fabricated in a compact form using standard integrated circuits. Automatic gain and threshold controls were provided so the optical input power could vary over a wide range. Clamping was employed to prevent baseline wander with an unbalanced data content of the signal, and timing was extracted by a phase-locked loop.

II. THEORY

A typical circuit for a photodiode driving an input amplifier is shown in Fig. 1(a) and its equivalent circuit in Fig. 1(b). The current generator i_d is the photo current. R_r is the dc return resistor for the detector, and i_r is the noise generator associated with it. The capacitor C_d is the

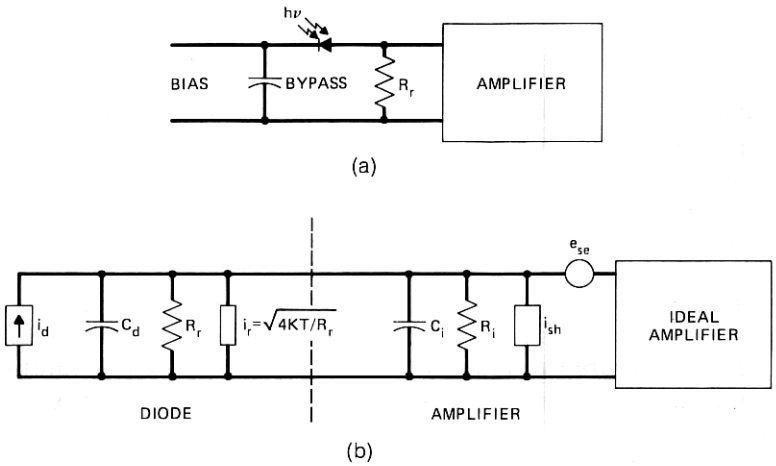

Fig. 1—(a) Input circuit. (b) Equivalent circuit.

output capacitance of the diode, C_i is the input capacitance to the amplifier (excluding feedback effects), and R_i is the input resistance of the amplifier. The quantities e_{se}^2 and i_{sh}^2 are the spectral noise densities of the series voltage and shunt current generators which characterize the noise properties of the amplifier.

A common approach to circuit design has been to set

$$\begin{aligned} \tau &= RC \\ &< 1/\text{baud rate}, \end{aligned}$$

where

$$R = \frac{R_r R_i}{R_r + R_i}$$

and

$$C = C_d + C_i$$

to minimize noise while not introducing significant intersymbol interference.

To achieve this, i_r and i_{sh} are often major sources of noise. Therefore, from the standpoint of noise, it is preferable to make R_r very large and employ an amplifier with low i_{sh}, even if $\tau \gg$ baud interval, to amplify the signal sufficiently to set the signal-to-noise ratio, and then to equalize the resulting distortion to eliminate intersymbol interference.

Two possible limitations to the high-impedance approach exist, both related to the low-frequency component of the signal developed across the detector. The difference in voltage between a long string of "ones" and a long string of "zeros" is proportional to the dc load resistance on the diode. Thus, the required dynamic range of the amplifiers preceding the equalizer increases with increasing R. Furthermore, with an avalanche detector this voltage could change the avalanche gain since it is in series with the diode bias. These two factors, which increase in importance as baud rate decreases, ultimately limit the magnitude of the detector load resistance.

In the remainder of this section the relationships between error rate, signal power, and the circuit parameters are discussed for a binary signal with both states equally likely. It is assumed that Gaussian noise statistics apply, that dark current is negligible, and that the amplifiers preceding the equalizer are linear.

Personick[5] has shown that for a pulse of average power p_o with avalanche gain of mean square $\langle g^2 \rangle$, if we assume the optical pulses are distinct, the ratio of the pulse peak to the root mean square thermal noise in the baseband circuit is equal to the ratio of the average cur-

rent of the received pulse to the square root of the quantity

$$I^2(p_o) = \frac{\eta e^2 p_0 f_b \langle g^2 \rangle}{h\nu} + n_t, \tag{1}$$

where n_t, the mean square thermal noise current* weighted to correct for input and output pulse shape, is given by

$$n_t = \left[\left(i_{sh}^2 + \frac{2kT}{R_r} + \frac{e_{se}^2}{R^2}\right) I_1 + (2\pi f_b C)^2 e_{se}^2 I_2\right] f_b. \tag{2}$$

The constants are

T = temperature
h = Plank's constant
ν = optical frequency
η = detector quantum efficiency
e = electron charge
f_b = bit rate.

The weighting functions I_1 and I_2, which take account of pulse shape, are given by

$$I_1 = \frac{f_b}{2\pi} \int_{-\infty}^{\infty} \left|\frac{H_{\text{out}}(\omega)}{H_p(\omega)}\right|^2 d\omega \tag{3}$$

$$I_2 = \frac{1}{(2\pi)^3 f_b} \int_{-\infty}^{\infty} \left|\frac{H_{\text{out}}(\omega)}{H_p(\omega)}\right|^2 \omega^2 d\omega, \tag{4}$$

where $H_{\text{out}}(\omega)$ is the Fourier transform of the output voltage pulse shape, $H_p(\omega)$ is the Fourier transform of the optical power pulse shape, and the pulses have been normalized so that the area of the optical pulse is unity, as is the magnitude of the output pulse at the center of the time slot. The functions I_1 and I_2 can be shown to depend only on pulse shape relative to the time slot length, not on baud rate.

The probability of error can be readily derived from eq. (1), assuming Gaussian noise statistics. For Gaussian-distributed noise, the probability that the noise current will exceed a value D is given by

$$P(D) = \frac{1}{2} \operatorname{erfc}\left(\frac{D}{I(p_o)\sqrt{2}}\right),$$

where erfc is the error function complement and I the root mean square

* Note that amplifier shot noise has been included in n_t.

noise current.[6] We assume an ideal regenerator where a "one" is produced if the input exceeds a threshold level D and a "zero" otherwise. Then if a "zero" is transmitted, the condition that the probability will be P_e that the noise will exceed the decision threshold is given by

$$D > QI(0), \tag{5}$$

where

$$Q = \sqrt{2}\ \mathrm{erfc}^{-1}\ (2P_e). \tag{6}$$

Similarly, so that the probability that the noise will not exceed the signal when a "one" is transmitted, the expected value of the signal, given by $p_{\max}\eta e\langle g\rangle/h\nu$, where $\langle g\rangle$ is the mean avalanche gain and $p_{\max}$ the average power for all "ones," must exceed the threshold by Q times the noise current; that is,

$$\frac{p_{\max}\eta e\langle g\rangle}{h\nu} - D > QI_{\max}. \tag{7}$$

From eqs. (1), (5), and (7), the average power required to achieve a specified error probability with avalanche gain is given by

$$p = \frac{h\nu Q}{2\eta}\left[\frac{Q\langle g^2\rangle f_b}{\langle g^2\rangle} + \frac{2}{\langle g\rangle e}\, n_t^{\frac{1}{2}}\right]; \tag{8}$$

where $\langle g^2\rangle$ is the mean square avalanche gain. (In the case without avalanche gain when thermal noise predominates, the first term in the bracket of eq. (8) can be neglected.) For avalanche photodiodes, it has been found that

$$\langle g^2\rangle = \langle g\rangle^{2+x} \tag{9}$$

and for silicon units $x = 0.5$.

A value of $\langle g\rangle$ exists which optimizes performance.[7] The value which minimizes the power required to achieve a given error rate, found by minimizing eq. (8), is given by

$$g_{\mathrm{opt}} = \frac{2^{4/3}}{(ef_bQ)^{\frac{1}{3}}}\, n_t^{\frac{1}{3}}. \tag{10}$$

At optimal gain the power required to achieve a specified error rate is given by

$$p = \frac{3h\nu Q}{\eta e g_{\mathrm{opt}}}\, n_t^{\frac{1}{2}} \tag{11}$$

$$p = \frac{3h\nu Q^{5/3} f_b^{\frac{2}{3}} n_t^{\frac{1}{2}}}{2^{4/3}\eta e^{\frac{1}{3}}}. \tag{12}$$

It is interesting to note that eq. (11) can also be put in the form

$$p = \frac{3}{g_{\text{opt}}} p', \tag{13}$$

where p' is the required power without avalanche gain. From eqs. (8), (10), and (12), the required power without avalanche gain, the optimum avalanche gain, and the required power with optimum avalanche gain are proportional to the second, third, and sixth roots of the thermal noise, respectively.

The series noise source of a junction field effect transistor (FET) is virtually independent of the circuit parameters in the normal range of operation, and the shunt noise source is negligible at 6.3 Mb/s without input tuning. For an FET[8]

$$e_{se}^2 \approx 2kT\left(\frac{0.7}{g_m}\right), \tag{14}$$

where g_m is the transconductance of the device, so the thermal noise referred to the detector is

$$n_t \approx 2kTf_b\left[\left(\frac{1}{R_r} + \frac{0.7}{g_m R^2}\right) I_1 + \frac{0.7(2\pi f_b C)^2}{g_m} I_2\right], \tag{15}$$

assuming all the noise is due to the first stage of the input amplifier. For a good FET the input resistance is virtually infinite, so

$$R = R_r.$$

In a common-source configuration, C is the sum of the drain-gate, gate-source, diode, and gate wiring capacitances.

III. CIRCUITRY

Figure 2 is a block diagram of the repeater, which was constructed in a $5\frac{1}{4} \times 4 \times 1\frac{1}{2}$ inch enclosure. The main signal path is represented by heavy lines and boxes. The signal, which is detected by either a PIN or a silicon avalanche photodiode, is first amplified by a high-impedance input amplifier. Following this, additional gain is provided by an SN52733 integrated video amplifier. Next, the signal is equalized, then further amplified by another SN52733 video amplifier and filtered by a single-section maximally flat LC filter with a 7-MHz bandwidth which, in combination with the other amplifiers, gives a 3-dB point of about 6.3 MHz. From this point the signal is fed to the timing circuits, the automatic gain and threshold circuits, and the regenerator. Finally, the regenerated signal is amplified and applied to the LED.

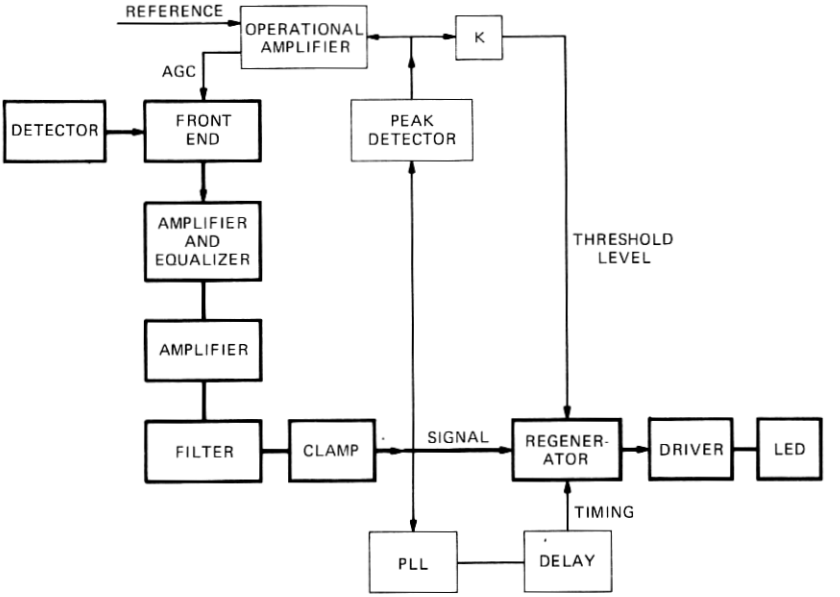

Fig. 2—6.3 Mb/s repeater.

3.1 Input amplifier

A 3-stage input amplifier was employed, as shown in Fig. 3. The amplifier consists of a 2N4416 junction field effect transistor followed by a 3N159 tetrode amplifier, and finally a 2N4416 in a source follower configuration. It was found experimentally that input amplifiers with a 2N4416 input stage had an input noise equivalent power about 1 dB less than with the 3N159. However, the tetrode can provide more gain for a single stage because of its low drain to first gate capacitance. Furthermore, the tetrode is well suited to automatic gain control since the g_m of the device is highly dependent on the voltage applied to the second gate. Thus, the configuration of Fig. 3 was chosen. It was found that the input noise dropped by 6 dB when the first gate of the tetrode was shorted to ground, so 75 percent of the thermal noise originates in the first stage. Thus, this configuration is very close to optimum. The source follower was provided to decouple the input amplifier from the subsequent circuits.

3.2 Equalization

In order to compensate for the distortion introduced by the long input time constant, the circuit of Fig. 4 was employed. With a source

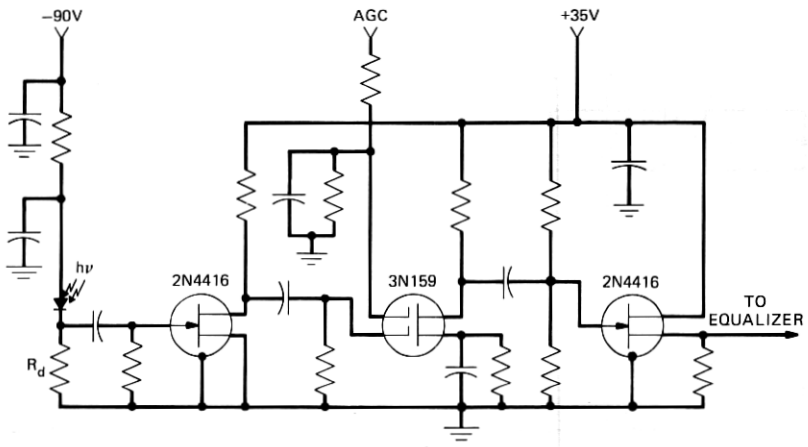

Fig. 3—Input amplifier.

of resistance R_s and a load whose resistance is included in R_2, it can be shown that the transfer function has a pole at

$$s = -\frac{1}{C_1 R_1}\left(1 + \frac{R_1}{R_s + R_2}\right)$$

and a zero at

$$s = -\frac{1}{C_1 R_1}.$$

Thus, the position of the zero can be adjusted by varying either C_1 or R_1 and, as long as

$$R_1 \gg R_s + R_2,$$

the pole will be above the band of interest and have a negligible effect.

3.3 Clamping and Peak Detection

Since the amplifiers of the repeater are ac-coupled, the dc level would be a function of word pattern unless suitable provisions are made.

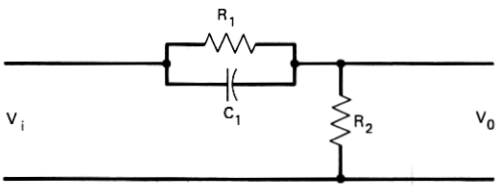

Fig. 4—RC equalizer.

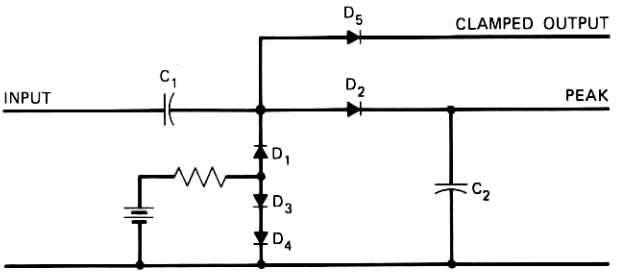

Fig. 5—Clamp and peak detector.

In addition, provision to measure signal level must be incorporated to set the threshold and to control gain. Clamping and peak detection were employed to solve these problems.

By incorporating both automatic threshold and gain controls, the AGC gain need only be high enough to assure that the phase-locked loop will function properly and to prevent compression. This reduces the tendency toward instability because of a high-gain feedback loop.

Figure 5 shows the circuit employed. Diode D_1 and capacitor C_1 serve as the clamp, and diode D_2 and capacitor C_2 serve as the peak detector. The diodes D_3, D_4, and D_5 are included to cancel the diode drops of D_1 and D_2.

3.4 Digital Circuits

The timing coincidence and regenerator circuits, Figs. 6 and 7, share an SN72810 dual comparator and an SN7474 dual D flip-flop. The comparator has the property

$$V_0 = 1, \qquad V_1 > V_2$$
$$V_0 = 0, \qquad V_1 < V_2,$$

where 1 and 0 represent states. For the D flip-flop, the output Q takes

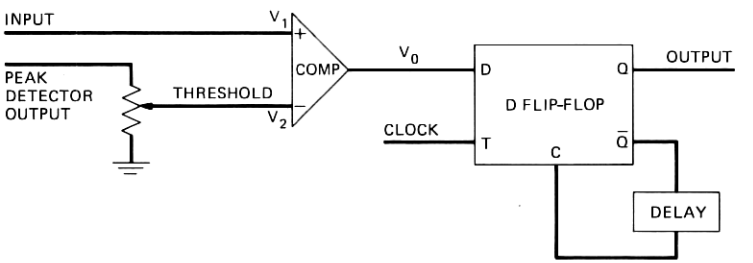

Fig. 6—Regenerator.

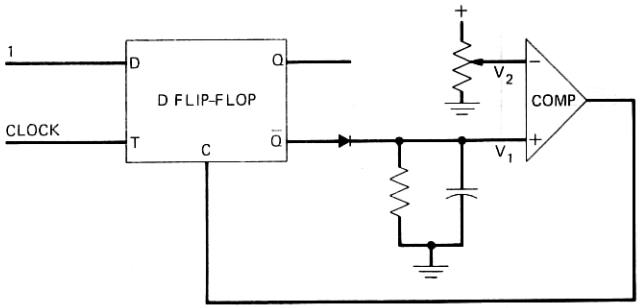

Fig. 7—Timing coincidence.

on the value applied to the D input when the clock input changes from low to high. This value is held until either the clock again shifts from low to high or the clear c is returned to ground. The output $\bar{Q}$ is the complement of Q.

In the regenerator, Fig. 6, the comparator serves as a quantizer and the D flip-flop retimes the signal. On the flip-flop, feedback from $\bar{Q}$ to c is provided so the D flip-flop output will be a pulse of proper duration whenever the clock goes positive and the D input is high.

The circuit shown in Fig. 7 is used to adjust timing coincidence between the phase-locked loop output and the regenerator. The D input to the flip-flop is kept high at all times. Adjusting the input to V_2 of the comparator adjusts the delay between the time when a positive clock pulse is applied and the voltage of the clear (c) drops to a sufficiently low value to clear the flip-flop. The rising edge of the $\bar{Q}$ output is used to trigger the regenerator.

3.5 LED and driver

The LED driver consists of a cascade of two emitter followers. The driver is capable of generating 1.5-A pulses into a diode load. For the tests to be described, the diode was driven with 300-mA peak current pulses and generated optical pulses of about 0.3-mW peak power.

IV. RESULTS

Both signal-to-noise ratio and error-rate measurements were made to evaluate the input amplifier and repeater performance. The 2N4416 JFET employed for all the tests had an input capacitance of 5 pF and g_m of 0.006 mho. An additional picofarad of capacitance was added by the diode load circuit. The measurements without gain were per-

formed with an SGD-040A PIN photodetector which had a capacitance of 2 pF and a quantum efficiency of 83 percent. For the measurements with gain, a TIXL56 silicon avalanche photodetector was employed. This diode had a capacitance of 1 pF and a quantum efficiency of 55 percent. For both diodes, the noise calculated from the measured dark current was negligible.

The constants I_1 and I_2 have been evaluated by Personick[5] for rectangular optical pulses and pulses with a raised cosine spectrum and maximum eye opening at the regenerator input. He found $I_1 = 0.6$ and $I_2 = 0.26$. The theoretical curves presented here were obtained using these values.

Measurements of noise equivalent power, that is, optical power to achieve a unity signal-to-noise ratio at the regenerator, were first made to evaluate the performance of the input amplifier. As shown in Fig. 8, the results for the input amplifier of Fig. 3 with equalization closely approximates those predicted from eq. (8) by setting $Q = 1$. The difference between the theoretical and the experimental curve is mainly due to the noise of the second stage, which was about 1 dB with the 1-MΩ diode load resistor.

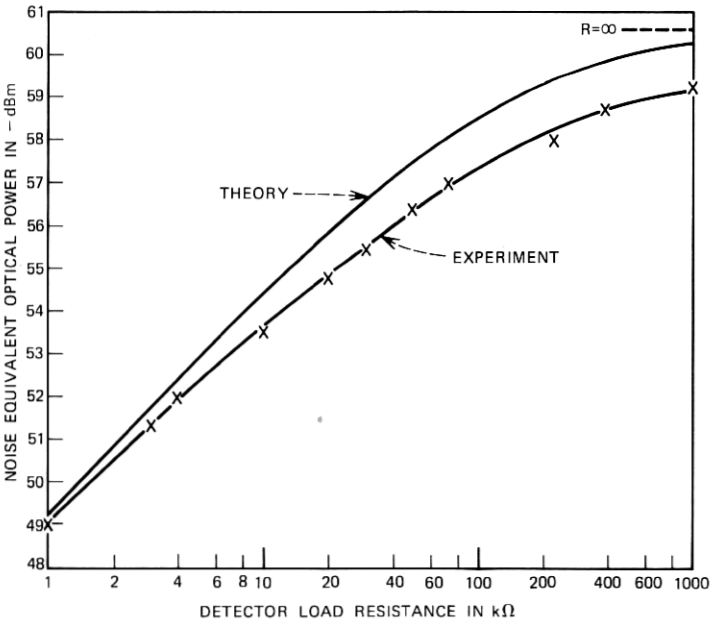

Fig. 8—Noise equivalent power circuit vs. diode load resistance.

Other input amplifiers were also tried. It was found that with a common-drain first stage and a common-source second stage, with a 1-MΩ diode load resistor, the noise equivalent power was about 1 dB higher. With smaller values of diode load resistance, where the resistor noise predominates, the common-drain input amplifier's performance was identical to that of the common-source input amplifier. Similar results were obtained with a cascade configuration using a bipolar transistor for the second stage.

Figure 9 shows "eye" diagrams taken at key points in the receiver with a 1-MΩ diode load resistance. Before equalization, the "eye" is fully closed, as is expected. After equalization, the "eye" is almost fully open. The regenerated pulse was photographed with recovered timing.

The tracking of the threshold level with peak signal is shown in Fig. 10. The tracking in conjunction with the AGC is adequate, as will be apparent from the error performance. With germanium or Schottky barrier diodes in the clamping and peak detection circuit, the tracking could have been held even closer to the ideal, had this been necessary. The AGC also functioned properly. The signal level could be held within about a 20-percent range with the power up to 10 dB above the signal required for 10^{-8} error probability. Greater range could be achieved by cascading tetrode FET stages, if required.

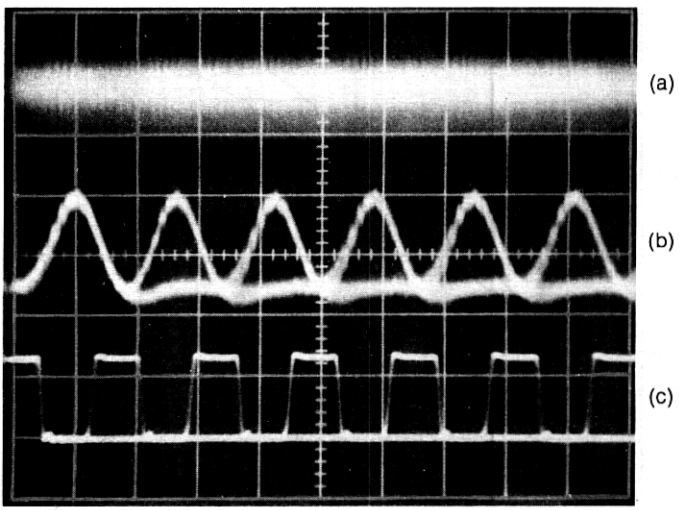

Fig. 9—"Eye" diagrams: (a) Before equalization. (b) After equalization. (c) Regenerated pulse.

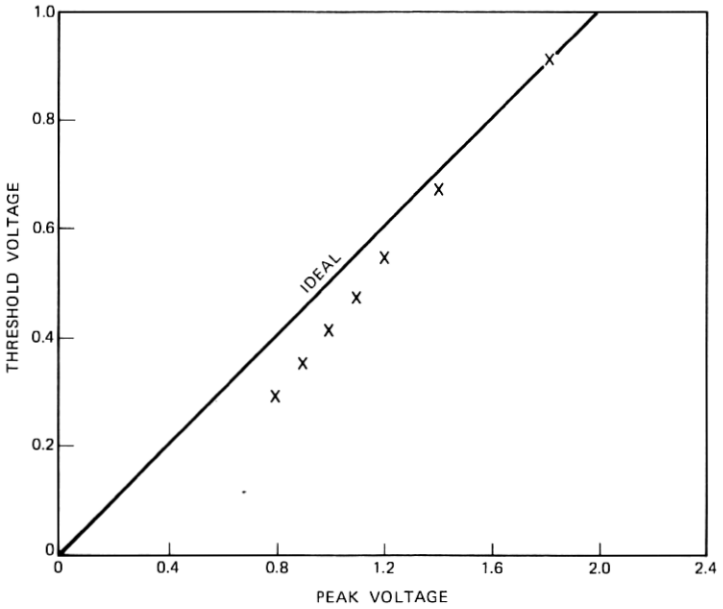

Fig. 10—Threshold voltage vs. peak voltage.

Error probability measurements were made under a variety of conditions. The results are shown in Fig. 11. The signal source was a 2^{15}-1 bit pseudo-random word generator. The signal consisted of 15 bit blocks each separated by a zero. The measurements were made with external timing and performance was optimized at each point, except the points indicated with x's. For these points, which were taken to check the performance of the automatic gain and threshold controls, as well as the timing recovery, the system was optimized with recovered timing and AGC at an error probability of about 10^{-8}. Then all the points were taken without further adjustment to the repeater.

The theoretical curve for a 4-kΩ diode load resistor is shown along with the measured points. These points were taken with the source-follower input amplifier because this amplifier introduced less intersymbol interference with the 4-kΩ diode load resistor. The improvement with a 1-MΩ diode load resistor over a 4-kΩ one was about 8 dB, which is in agreement with the theory.

Measurements of repeater performance were made with a TIXL56 silicon avalanche photodiode. This diode exhibits a significant diffusion tail. A second stage of RC equalization was employed to remove the resulting intersymbol interference.

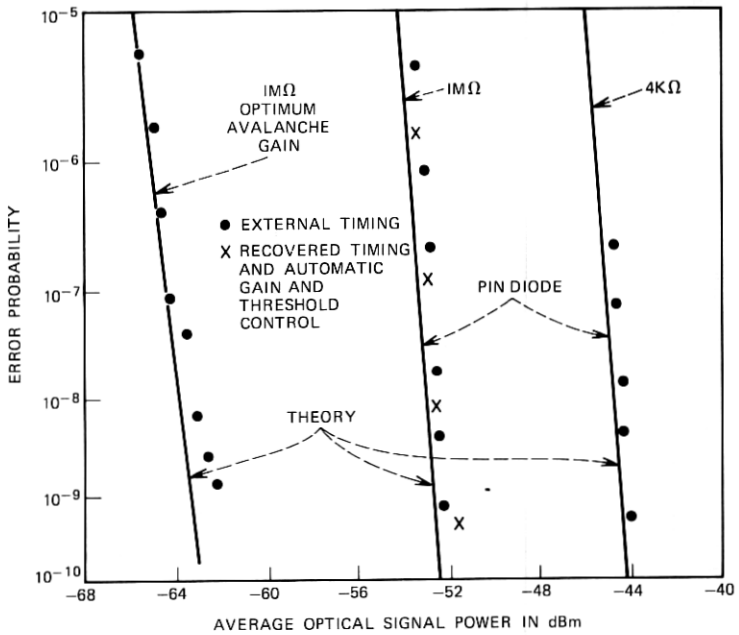

Fig. 11—Error probability vs. average optical signal power.

Equation (10) indicates that the optimum avalanche gain is a function of error rate. However, since it is not practical to optimize the gain at extremely low error probability, the gain was optimized at an error probability of 5×10^{-7} and then held constant for all the points.

Table I shows a comparison of the measured and predicted values of g_{opt} for 4-kΩ and 1-MΩ diode load resistance. In view of the assumption of noise statistics and diode characteristic, the agreement is satisfactory.

V. CONCLUSIONS

It has been demonstrated that a simple compact low-cost* repeater suitable for fiber optic applications can be built which functions close to theory at 6.3 Mb/s. The high-impedance input amplifier and its associated equalizer were realized in a straightforward manner, and compression did not turn out to be a serious problem. A significant reduction in required signal power to achieve a specified error rate with-

* The cost of the active components was about $30, exclusive of the detector and LED. An SGD-040 PIN detector costs about $15 and a TIXL56 avalanche detector $65.

Table I

Detector Load Ohms	Theoretical Gain	Measured Gain
4 K	171	188
1 M	44	62.2

out avalanche gain was achieved. With an avalanche detector, the optimum gain was greatly reduced with high impedance input, as predicted. Thus, the temperature stability will be greatly increased and the diode fabrication requirements eased with an avalanche detector.

VI. ACKNOWLEDGMENT

The author wishes to acknowledge the advice and assistance of W. M. Muska in the fabrication of the repeater.

REFERENCES

1. D. B. Keck, P. C. Schultz, and F. Zimar, "Attenuation of Multimode Glass Optical Waveguide," Appl. Phys. Lett., *21*, No. 5 (September 1, 1972).
2. A. B. Gillespie, *Signals, Noise, and Resolution in Nuclear Counter Amplifiers*, New York: McGraw-Hill, 1953.
3. O. H. Schade, Sr., "A Solid-State Low-Noise Preamplifier and Picture-Tube Drive Amplifier for a 60 mHz Video System," RCA Review, *29*, No. 1 (March 1968), p. 3.
4. C. A. Burrus and R W. Dawson, "Small-Area High-Current GaAs Electroluminescent Diodes and a Method of Operation for Improved Degradation Characteristics," Appl. Phys. Lett., *17*, No. 3 (August 1970), pp. 97–99.
5. S. D. Personick, "Receiver Design for Digital Fiber Optic Communication Systems, Pt. I," B.S.T.J., *52* (July 1973), pp. 843–886.
6. W. R. Bennett and J. R. Davey, *Data Transmission*, New York: McGraw-Hill, 1965, pp. 100, 101.
7. H. Melchior and W. T. Lynch, "Signal and Noise Response of High Speed Germanium Avalanche Photodiodes," IEEE Trans. on Elec. Devices, *ED 13*, No. 12 (December 1966), pp. 829–838.
8. A. van der Ziel, *Noise, Sources, Characterization, Measurement*, Englewood Cliffs, N.J.: Prentice-Hall, 1970, pp. 74–76.